Available online at www.sciencedirect.com
ScienceDirect
Ceramics International 37 (2011) 2323–2328
CERAMICS INTERNATIONAL
www.elsevier.com/locate/ceramint

The luminescence spectroscopy and thermal stability of red-emitting phosphor $Ca_9Eu(VO_4)_7$

Xiao Wu [a], Yanlin Huang [a,*], Hyo Jin Seo [b,*]

[a] College of Chemistry, Chemical Engineering and Materials Science, Soochow University, Suzhou 215123, China
[b] Department of Physics, Pukyong National University, Busan 608-737, Republic of Korea

Received 5 February 2011; received in revised form 15 March 2011; accepted 18 March 2011
Available online 29 March 2011

Abstract

Eu-based vanadate $Ca_9Eu(VO_4)_7$ phosphor was synthesized by the solid state reaction method and was characterized by X-ray powder diffraction (XRD). The photoluminescence excitation and emission spectra, fluorescence decay curves and the dependence of luminescence intensity on temperature were investigated. The phosphor can be efficiently excited by near UV light to realize an intense red luminescence (614 nm) corresponding to the electric dipole transition $^5D_0 \rightarrow {}^7F_2$ of Eu^{3+} ions. The crystallographic site-occupations of the Eu^{3+} ions in $Ca_9Eu(VO_4)_7$ were investigated by the site-selective excitation and emission spectra, and the fluorescence decay curves in the $^5D_0 \rightarrow {}^7F_0$ region using a pulsed, tunable, narrowband dye laser. The red luminescence together with the thermal stability was discussed on the base of the Eu^{3+} site-distribution in $Ca_9Eu(VO_4)_7$ host.

Keywords: A. Powders: chemical preparation; B. Chemical synthesis; C. Optical properties

1. Introduction

The red-emitting materials usually can be achieved by doping the line-emitting ions in a host, such as Pr^{3+}, Sm^{3+}, and Eu^{3+} ions [1–5]. In particular, Eu^{3+}-doped phosphors are popularly used for the application in near UV and white light emission diodes (LEDs), since they exhibit high quantum efficiency and photo-stability. Accordingly, the investigations of luminescence in Eu^{3+} ions doped hosts have gained much attention in recent years [6–10].

For example, Eu^{3+}-doped vanadium oxides have been paid much attention for applications in display devices, lighting and detectors in the past years. Usually, vanadate compounds have broad and intense charge transfer (CT) absorption bands from oxygen to metal ions in the near UV wavelength region. Under UV excitation, the CT band of vanadate host can transfer the excitation energy to the luminescent center by a nonradiative transition process [11].

In general, the temperature dependence of phosphors used in phosphor-converted white LEDs is important because it has great influence on the light output and color rendering index. The junction temperature of typical LEDs can be higher than 100 °C. There are significant thermal quenching of phosphors and emission color shift at $T > 100$ °C [12]. However, the obvious drawback of many Eu^{3+} doped vanadates is the thermal-quenching of luminescence at high temperature. For example, Setlur et al. [12] have reported that the red luminescence of Eu^{3+} doped $Ca_2NaMg_2V_3O_{12}$ can provide a high-quality white emission spectrum from the single phosphor. And Yamamoto et al. have reported that the luminescence of $EuNa_2Mg_2(VO_4)_3$ is six times as bright as that of YVO_4:Eu^{3+} under 365 nm light excitation at room temperature [13]. However, they all suffer from thermal quenching at higher temperatures. The significant thermal quenching and changes in the emission color at higher temperatures probably prevent the use of this phosphor in UV-LED packages because of the difficulty in maintaining constant phosphor color with either device or ambient temperature. Usually, the quenching could be attributed to the non-radiative relaxation from the emitting states related to the site-occupations of Eu^{3+} ions. For example, the disordered distribution of Eu^{3+} and Na^+ in

* Corresponding authors.
E-mail addresses: Huang@suda.edu.cn, huangyanlin@hotmail.com (Y. Huang), hjseo@pknu.ac.kr (H.J. Seo).

0272-8842/$36.00
doi:10.1016/j.ceramint.2011.03.031

$EuNa_2Mg_2(VO_4)_3$ was also considered to induce the thermal quenching. Similar strong quenching was also observed in other disordered compounds, such as $EuK_5(MoO_4)_4$ and $EuA(MoO_4)_2$ (A = Na, K, and Rb) [13]. Consequently, the selection of the host materials and the fundamental understanding of energy transfer within phosphors are important.

In this work, $Ca_9Eu(VO_4)_7$ with whitlockite-like structure was synthesized by the conventional high temperature solid state reaction. The phosphor was characterized by X-ray diffraction (XRD), photoluminescence excitation and emission spectra. The dependence of luminescence and the color coordinates on temperatures were evaluated for the potential application of this phosphor. The site-selective excitation and emission spectra together with fluorescence decay curves were also investigated. The crystallographic sites of Eu^{3+} in this host were discussed to elucidate its luminescence quenching with the elevated temperatures.

2. Experimental

Polycrystalline sample $Ca_9Eu(VO_4)_7$ was synthesized by using a conventional solid-state reaction. The starting material was a stoichiometric mixture of reagent grade ammonium vanadate (NH_4VO_3), europium oxide (Eu_2O_3), and calcium carbonate ($CaCO_3$). Firstly, the stoichiometric mixture was slowly heated up to 350 °C in 7 h and kept at this temperature for 5 h. The obtained powder was mixed again and then heated up to 700 °C for 5 h in air. After that, the sample was thoroughly mixed and heated at 1000 °C for 10 h in air.

The XRD pattern was collected on a Rigaku D/Max diffractometer operating at 40 kV, 30 mÅ with Bragg–Brentano geometry using Cu Kα radiation (λ = 1.5405 Å) and analyzed by using Jade-5.0 software Program. Photoluminescence excitation spectra and UV-excited luminescence spectra were recorded on a Perkin-Elmer LS-50B luminescence spectrometer with Monk–Gillieson type monochromators and a xenon discharge lamp used as excitation source. To study thermal quenching from 20 to 150 °C, the same spectrofluorimeter was equipped with a homemade heating cell under the excitation of a 365 nm UV lamp.

For the excitation and site-selective emission measurements, the excitation source was a dye laser (Spectron Laser Sys. SL4000) pumped by the second harmonic (532 nm) of a pulsed Nd:YAG laser (Spectron Laser Sys. SL802G). The pulse energy was about 5 mJ with 10 Hz repetition rate and 5 ns duration. The luminescence was dispersed by a 75 cm monochromator (Acton Research Corp. Pro-750) and observed with a photomultiplier tube (Hamamatsu R928). The excitation spectra of the $^7F_0 \rightarrow {}^5D_0$ transition were obtained by monitoring total luminescence by setting the monochromator in zero order of diffraction to pass all the $^5D_0 \rightarrow {}^7F_J$ (J = 1, 2, 3 and 4) emission in which a 580 nm cutoff filter was used. Time-integrated signals from a digital storage oscilloscope (LeCroy 9310A) were recorded for the emission and excitation spectra under pulsed laser excitation.

3. Results and discussion

3.1. The crystal phase

Fig. 1 shows the XRD patterns of $Ca_9Eu(VO_4)_7$ polycrystalline and the JCPDS Card No. 45-0549. By a comparison between them, the position and the relative intensities of the main peaks are the same. The unit cell lattice parameters of $Ca_9Eu(VO_4)_7$ are calculated to be a = 10.869 Å, c = 38.096 Å, $\alpha = \beta = 90^\circ$ and $\gamma = 120^\circ$. These crystallographic parameters are similar to those of $Ca_9Nd(VO_4)_7$ [14] and $Ca_9Dy(VO_4)_7$ [15]. The XRD analysis demonstrates that $Ca_9Eu(VO_4)_7$ shows whitlockite-type hexagonal structure with the space group of *R3c* (161) [16,17].

3.2. The photoluminescence emission spectra

The excitation spectrum of $Ca_9Eu(VO_4)_7$ obtained by monitoring the $^5D_0 \rightarrow {}^7F_2$ at 614 nm is shown in Fig. 2(a), which consists of two broad excitation peaks in the regions between 200 and 350 nm together with some emission lines. From the viewpoint of molecular orbital theory, the three bands (about 265, 301 and 318 nm) correspond to electric or magnetic dipole allowed transitions from the $^1A_2(^1T_1)$ ground state to $^1E(^1T_2)$, $^1A_1(^1E)$ and $^1B_1(^1E)$ excited states of VO_4^{3-} ions, respectively [18]. We have clearly illustrated that this broad excitation (200–350 nm) was due to the absorption of VO_4^{3-} group in $Ca_9Dy(VO_4)_7$ host [13]. This indicates that the transfer energy can be taken place efficiently from the VO_4^{3-} to Eu^{3+} ions in $Ca_9Eu(VO_4)_7$. This is similar to the energy transfer of $VO_4^{3-} \rightarrow Eu^{3+}$ in YVO_4 [19]. However, the charge transfer band of Eu^{3+}–O^{2-} is also possible to overlap in the broad band at 270 nm in Fig. 2(a).

The excitation spectra have some dominated sharp lines in the wavelength region of 350–500 nm due to the f–f transitions within $4f^9$ configuration of Eu^{3+} ions. Many kinds of Eu^{3+} doped materials have been investigated to develop the red-emitting phosphors for white LEDs. A suitable red-emitting UV-LED phosphor should exhibit absorption around 400 nm

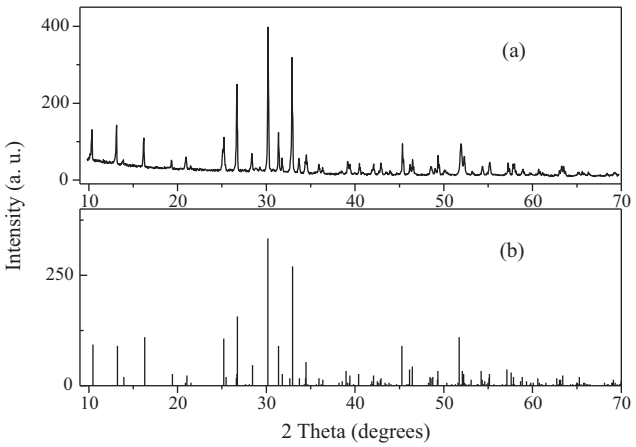

Fig. 1. The XRD patterns of $Ca_9Eu(VO_4)_7$ in this work (a), and JCPDS Card No. 45-0549 (b).

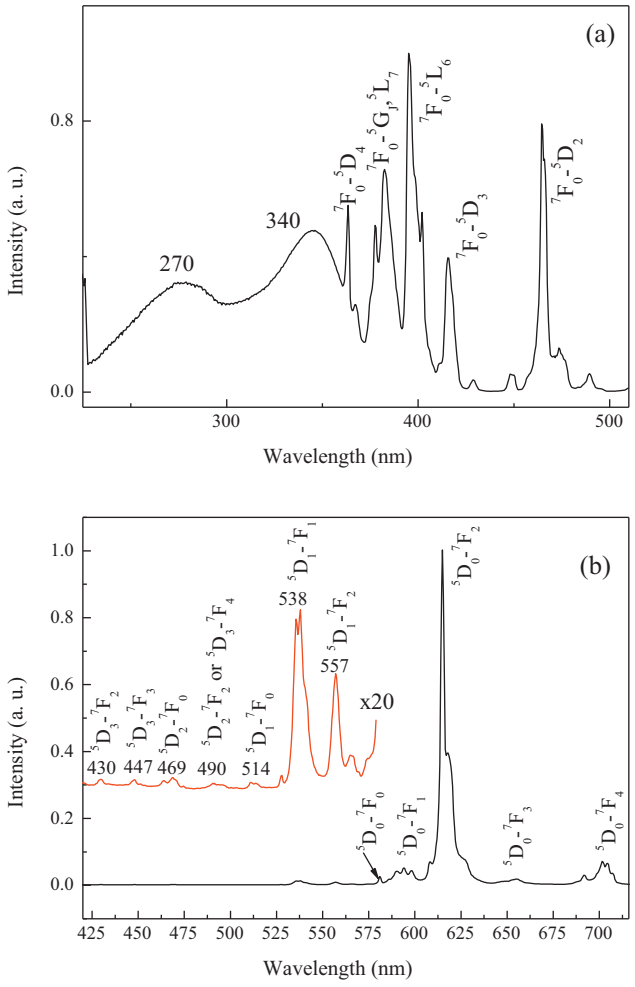

Fig. 2. The excitation (a, λ_{em} = 614 nm) and emission (b, λ_{ex} = 395 nm) spectra of the $Ca_9Eu(VO_4)_7$ at 300 K.

(LED excitation wavelength). Obviously, the excitation spectrum (Fig. 2, a) indicates that $Ca_9Eu(VO_4)_7$ can be efficiently excited by the radiation of near UV-emitting InGaN based LED chips.

Fig. 2(b) presents the emission spectra of $Ca_9Eu(VO_4)_7$ excited by 395 nm. The $Ca_9Eu(VO_4)_7$ phosphor shows bright red color and the intensity is 3.9 times higher than that of Y_2O_2S:0.05Eu^{3+} under the same conditions (figure omitted). The emission peaks at about 580 and 590 nm are derived from the transitions of $^5D_0 \rightarrow {}^7F_0$ and $^5D_0 \rightarrow {}^7F_1$, respectively. The emission intensities corresponding to the transitions of $^5D_0 \rightarrow {}^7F_{3,4}$ are weak. The dominant red emission of 614 nm is attributed to the electric dipole transition $^5D_0 \rightarrow {}^7F_2$, indicating that Eu^{3+} is located at the site of non-inversion symmetry. This is in good agreement with the crystal structure. The compound $Ca_9Eu(VO_4)_7$, like most whitlockites, has the $Ca_3(VO_4)_2$ or β-$Ca_3(PO_4)_2$ structure with no inversion center [17]. Consequently, $^5D_0 \rightarrow {}^7F_2$ red emission (614 nm) presents the most prominent intensity in the emission spectrum.

It is well known that the forced electrical dipole transition $^5D_0 \rightarrow {}^7F_2$ is very sensitive to the local environment, while the magnetic dipole transition $^5D_0 \rightarrow {}^7F_1$ is not much affected by the ligand field around Eu^{3+}. Therefore, the intensity ratio of $R = I(^5D_0 \rightarrow {}^7F_2)/I(^5D_0 \rightarrow {}^7F_1)$ is a measure of rare-earth ion site symmetry [20]. A lower symmetry of the crystal field around Eu^{3+} will result in a higher value of R. The intensity ratio R of $Ca_9Eu(VO_4)_7$ is 10, which is quite large in comparison with that of other Eu^{3+}-doped phosphors.

In the emission spectrum (Fig. 2, b), except for the emission lines from the lowest excited $^5D_0$ level of Eu^{3+}, the transition lines from the higher energy levels ($^5D_1$, $^5D_2$, and $^5D_3$) of Eu^{3+} are observed with weak intensity. The locations of the emission lines of Eu^{3+} and their assignments are indicated in Fig. 2. The presence of emission lines from higher excited states of Eu^{3+} ($^5D_1$, $^5D_2$, and $^5D_3$) are attributed to the low vibration energy of $(VO_4)^{3-}$ groups (823 cm^{-1}) [19]. The multiphonon relaxation by $(VO_4)^{3-}$ is not enough to bridge the gaps between the higher energy levels ($^5D_1$, $^5D_2$, and $^5D_3$) and the $^5D_0$ level of Eu^{3+} completely, resulting in weak emissions from these levels. In other Eu^{3+}-doped oxides, e.g., silicate and borates with maximum vibration energy of 1000–1200 cm^{-1}, such emissions cannot be detected [21].

The decay curves measured for the $^5D_0$ and $^5D_1$ states can well separated them. As shown in Fig. 3, the luminescence from

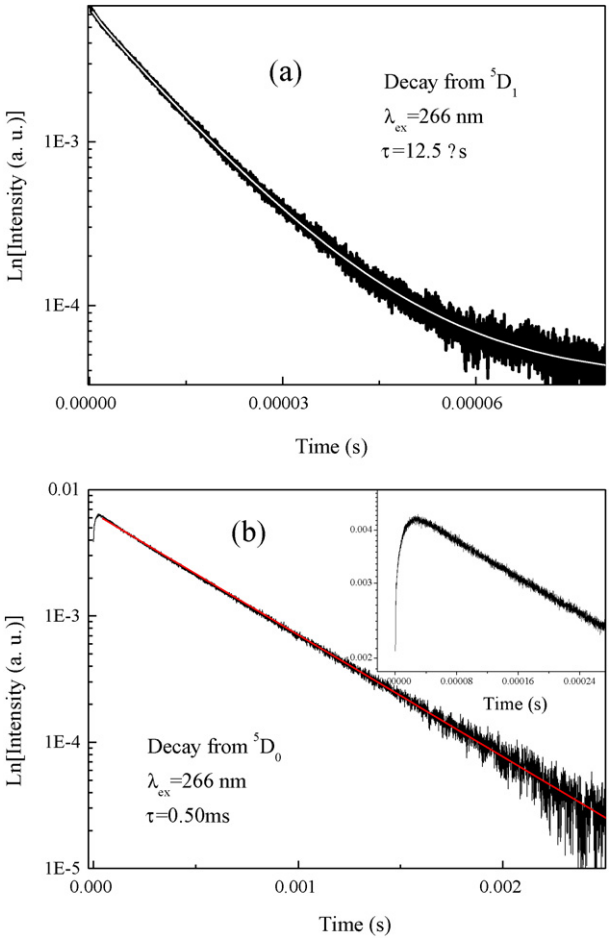

Fig. 3. The representative luminescence decay curves of $^5D_1$ (a, by monitoring the emission at 538 nm) and $^5D_0$ (b, by monitoring at 614 nm). The inset in (b) is the enlargement of the decay. The excitation is using 266 nm Nd:YAG pulsed laser.

$^5D_1$ presents a fast decay with a non-exponential profile under the excitation of 266 nm pulsed Nd:YAG laser. This suggests the presence of thermally activated energy transfer process. The lifetime value can be given to the average lifetime defined as:

$$\tau_{\text{average}} = \frac{\int tI(t)dt}{\int I(t)dt} \quad (1)$$

The lifetime of Eu^{3+} ($^5D_1$) is determined as 12.5 μs. However, the decay of the $^5D_0$ state shows single exponential and yields a long decay time of 0.5 ms. The rise time (see inset of Fig. 3(b)) observed at the beginning of the decay profile allows to infer that the $^5D_0$ state is mainly populated by relaxation from the upper states.

3.3. The dependence of luminescence intensities on temperature

Fig. 4 shows the temperature dependent luminescence spectra of $Ca_9Eu(VO_4)_7$. The luminescence intensities keep nearly constant from 20 to 60 °C. Then the emission decreases slowly with increasing temperature to 150 °C (decreases by about 18% of the initial value at 20 °C) (inset in Fig. 4). In addition, the emission wavelengths show no shifts with increasing temperature from 20 to 150 °C. Fig. 5 shows the CIE (1931) chromaticity coordinates of $Ca_9Eu(VO_4)_7$ from 20 to 150 °C. With increasing temperature, the color coordinates of the phosphor have no changes. The CIE values keep the value of about ($x = 0.65$, $y = 0.35$), which are all closer to the standard of NTSC ($x = 0.67$, $y = 0.33$) than that of commercial red phosphor of $Y_2O_2S:Eu^{3+}$ ($x = 0.622$, $y = 0.351$) [22].

Compared with the reported "stoichiometric" concentrated vanadate (such as $EuNa_2Mg_2(VO_4)_4$), or a "doped material" ($Ca_2NaMg_2V_3O_{12}$ or $YNa_2Mg_2(VO_4)_4$), $Ca_9Eu(VO_4)_7$ phosphor has two improvements on the temperature quenching effect, i.e., excellent thermal stability of luminescence intensity and stable color (no emission shift).

The mechanisms of the thermal instability in Eu^{3+}-doped samples are complicated. The temperature-quenching effect of

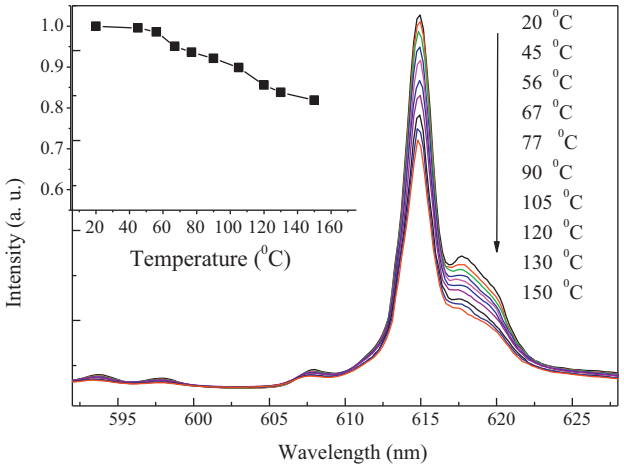

Fig. 4. The emission spectra of $Ca_9Eu(VO_4)_7$ under the excitation of 365 nm at different temperatures. The inset shows the integrated luminescence intensities normalized at 20 °C.

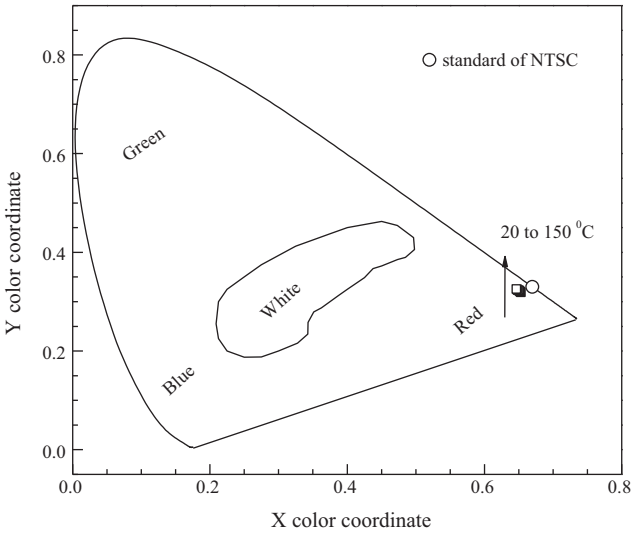

Fig. 5. CIE (1931) chromatic coordinates of $Ca_9Eu(VO_4)_7$ phosphor calculated from the emission spectra at 20–150 °C in Fig. 4.

Eu^{3+} luminescence becomes strong with the elevated temperature, which is generally due to energy migration and transfer to nonradiative traps and Eu^{3+} within the host lattice. It should be necessary to investigate the microstructure of the distribution of Eu^{3+} in the $Ca_9Eu(VO_4)_7$ host.

3.4. The excitation spectra of $^7F_0 \rightarrow {}^5D_0$ transition

To examine the details of the site distributions of Eu^{3+} ions in $Ca_9Eu(VO_4)_7$ the excitation spectra corresponding to the $^7F_0 \rightarrow {}^5D_0$ transition were investigated by monitoring the total luminescence in Fig. 6. The excitation spectra in the $^7F_0 \rightarrow {}^5D_0$ transitions are separated to three main excitation peaks at 578.6, 579.7 and 580.1 nm. No other line corresponding to the $^7F_0 \rightarrow {}^5D_0$ transition could be detected. The $^7F_0$ ground state and the $^5D_0$ excited state are non-degenerate and they cannot be split by the crystal field surrounding the Eu^{3+} ions. The

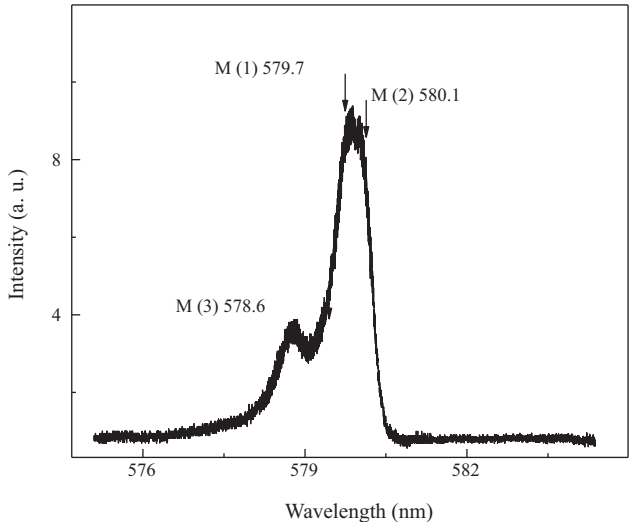

Fig. 6. The excitation spectra for $^7F_0 \rightarrow {}^5D_0$ transition of Eu^{3+} in $Ca_9Eu(VO_4)_7$ by monitoring the total luminescence.

presence of three $^5D_0 \rightarrow {}^7F_0$ transitions confirms that the Eu^{3+} ions are doped into the $Ca_9Eu(VO_4)_7$ matrix in three crystallographic sites.

In the initial $Ca_3(VO_4)_2$ and β-$Ca_3(PO_4)_2$, Ca^{2+} ions occupy five independent sites: *M*1, *M*2, *M*3, *M*4 and *M*5. The *M*1, *M*2, and *M*3 (18*b*) and *M*5 (6*a*) sites are fully occupied while the *M*4 site (6*a*) is half-occupied. There is one vacant site, *M*6 (6*a*), in the structure [23]. The site occupancies by rare-earth metal ions change monotonically with decreasing radii from La^{3+} to Lu^{3+}.

It has been well investigated that two groups of rare-earth metals have been selected depending on this distribution. The first group includes rare-earth metals from La^{3+} to Eu^{3+}, and the second group includes rare-earth metals from Gd^{3+} to Lu^{3+} and Y^{3+} [14]. In the first group, La^{3+}–Eu^{3+} ions are distributed among the *M*1, *M*2, and *M*3 sites together with the Ca^{2+} ions. In the second group, Gd^{3+}–Lu^{3+} and Y^{3+} ions are located at the *M*1, *M*2, and *M*5 sites together with the Ca^{2+} ions. $Ca_9Eu(VO_4)_7$ is isotypic with $Ca_3(VO_4)_2$ and β-$Ca_3(PO_4)_2$ and belong to the first group [24]. The presence of three $^7F_0 \rightarrow {}^5D_0$ transitions in Fig. 6 is agreed with this conclusion, and the three site positions of Eu^{3+} ions are in good agreement with the results recently reported by Benhamou et al. [25] They confirmed similar three site-distributions of Eu^{3+} in $Ca_9Eu(PO_4)_7$ at 578.5, 579.5, 580.1 nm for the *M*3, *M*1 and *M*2 sites, respectively, by means of X-ray diffraction and low temperature Eu^{3+} luminescence studies [25]. Following this conclusion, it could be suggested that in $Ca_9Eu(VO_4)_7$, there are three cation positions occupied by Eu^{3+}: *M*3 (578.65 nm), *M*1 (579.7 nm) and *M*2 (580.1 nm) as shown in Fig. 6.

3.5. The site-selective emission and decay curves

The site-selective emission spectra were recorded by tuning the laser to resonance with each excitation peaks of site *M*3 (578.6 nm), *M*1 (579.7 nm) and *M*2 (580.1 nm) (labeled in Fig. 6) at 300 K. The three spectra in Fig. 7 have nearly the same profile with the same emission wavelength position for site-selectively excitation into three single sites. The strongest emission line is the $^5D_0 \rightarrow {}^7F_2$ transition at 614 nm for three sites. Actually, this characteristic can also be supported by the fluorescence decay for each site. Fig. 8 shows decay curves of $^5D_0 \rightarrow {}^7F_2$ emissions under excitation in sites *M*3 (578.6 nm), *M*1 (579.7 nm) and *M*2 (580.1 nm). The curves can be fitted into a single exponential function as:

$$I = I_0 \exp\left[-\frac{t}{\tau}\right], \tag{2}$$

where I_0 is the initial emission intensity for $t = 0$, τ is the lifetime. The luminescence from *M*3 (578.6 nm), *M*1 (579.7 nm) and *M*2 (580.1 nm) sites exhibit the same lifetime of 0.51 ms.

In rare earth compounds, G. Blasse explained the energy transfer processes between identical centers (*S*) [26]. Usually, if the transfer between two ions *S* occurs with high rate, the transfer can occur in the first step and be followed by many others. This can bring the migration of excitation energy. If in this way the excitation energy reaches a site where it is lost nonradiatively (a killer or quenching site), the luminescence will be quenched [12]. If the excitation into *S* is followed by emission from the same kind of *S* ion, or if any energy migration can take place and the excitation into *S* is followed after some migration by emission from *S* only, the decay can be described by the function

$$I = I_0 \exp(-rt) \tag{3}$$

where I_0 is the emission intensity at time $t = 0$, and r is the radiative rate. In this case, the donor–donor transfer is very rapid and the luminescence also keeps single-exponential decay [26].

According to the results above there are three cation positions of Eu^{3+} ions in the stoichiometric host lattices of $Ca_9Eu(VO_4)_7$, i.e., *M*3 (578.65 nm), *M*1 (579.7 nm) and *M*2 (580.1 nm), which present nearly the same emission and decay. It can be suggested that in $Ca_9Eu(VO_4)_7$ the three positions of the Eu^{3+} ions were arranged in the sites with similar environment. Actually, the crystal fields of the *M*1, *M*2 and *M*3 are almost the same due to a slight difference in bond

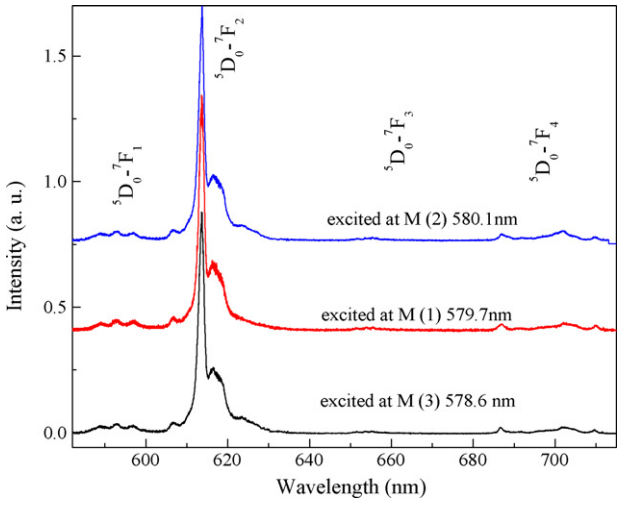

Fig. 7. The site-selective emission spectra of $^5D_0 \rightarrow {}^7F_J$ (J = 1, 2, 3, 4) for $Ca_9Eu(VO_4)_7$ by exciting into site *M*1: 579.7 nm, *M*2: 580.1 nm, and *M*3: 578.6 nm.

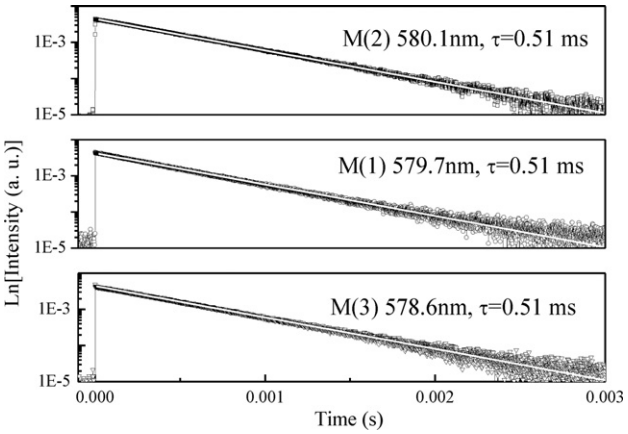

Fig. 8. The $^5D_0 \rightarrow {}^7F_2$ luminescence decay curves under the excitation of site *M*1 at 579.7 nm, *M*2: 580.1 nm, and *M*3: 578.6 nm.

lengths from cation to oxygen in $Ca_9R(VO_4)_7$ (R = rare earth ions) [27]. In the fully concentrated Eu-compound, the emission occurs after diffusion between both identical and different sites resulting in the same spectral feature and decay behavior. Therefore the identical spectra and decays are due to the averaged properties between Eu^{3+} ions at different sites. This structure characteristic can be suggested to be responsible for the strong luminescence and stable thermal quenching in $Ca_9Eu(VO_4)_7$. Yamamoto et al. [13] have suggested that the disordered distribution of Eu^{3+} in a concentrated Eu-compound is responsible for the thermal quenching. For example, the strong quenching of luminescence were observed in $EuNa_2Mg_2(VO_4)_3$, $EuK_5(MoO_4)_4$ and $EuA(MoO_4)_2$ (A = Na, K and Rb) [13]. The knowledge of the site-distribution over the different sites in a host structure will be useful to deeply analyze the luminescence mechanisms [25].

4. Conclusions

A red-emitting phosphor was synthesized by the solid state reaction method. The excitation spectrum consists of a broad band ranging from 200 to 350 nm due to the absorption of VO_4^{3-} group together with the strong f–f transitions of Eu^{3+} ions. $Ca_9Eu(VO_4)_7$ can be efficiently excited by the radiation of near UV-emitting InGaN based LED chips. The phosphor shows intense red emission from the electric dipole transition $^5D_0 \rightarrow {}^7F_2$, which shows high quenching temperature and stable color purity with the elevated temperature. The excitation spectra corresponding to $^7F_0 \rightarrow {}^5D_0$ transition show three site distributions of Eu^{3+} in $Ca_9Eu(VO_4)_7$: $M3$ (578.6 nm), $M1$ (579.7 nm) and $M2$ (580.1 nm). The three sites present nearly the same emission spectra and decay lifetime under the site-selectively excitation for each site. In $Ca_9Eu(VO_4)_7$, the Eu^{3+} ions are distributed in the stoichiometric host with a highly similar environment. This could be a possible reason for the strong luminescence and thermal stability of the Eu^{3+} in this phosphor.

Acknowledgements

This work was supported by Mid-career Researcher Program through National Research Foundation (NRF) grant funded by the Ministry of Education, Science and Technology (MEST) (No. 2009-0078682).

References

[1] R.M. Krsmanović, Ž. Antić, M.G. Nikolić, M. Mitrić, M.D. Dramićanin, Preparation of Y_2O_3:Eu^{3+} nanopowders via polymer complex solution method and luminescence properties of the sintered ceramics, Ceram. Int. 37 (2011) 525–531.

[2] K. Park, S.W. Nam, M.H. Heo, VUV photoluminescence properties of $Y_{1-x}Gd_xVO_4$:Eu phosphors prepared by ultrasonic spray pyrolysis, Ceram. Int. 36 (2010) 1541–1544.

[3] Y. Yu, D. Chen, P. Huang, H. Lin, Y. Wang, Structure and luminescence of Eu^{3+} doped glass ceramics embedding ZnO quantum dots, Ceram. Int. 36 (2010) 1091–1094.

[4] G. Bhaskar Kumar, S. Buddhudu, Synthesis and emission analysis of RE^{3+} (Eu^{3+} or Dy^{3+}):Li_2TiO_3 ceramics, Ceram. Int. 35 (2009) 521–525.

[5] M.H. Hwang, Y.J. Kim, Luminescent properties of Eu^{3+}-doped $YTaO_4$ powders, Ceram. Int. 34 (2008) 1117–1120.

[6] R.Y. Yang, H.Y. Chen, C.M. Hsiung, S.J. Chang, Crystalline morphology and photoluminescent properties of $YInGe_2O_7$:Eu^{3+} phosphors prepared from microwave and conventional sintering, Ceram. Int. 37 (2011) 749–752.

[7] T.W. Kuo, T.M. Chen, Synthesis and luminescence properties of Eu^{3+}, Ce^{3+} and Tb^{3+}-activated $Sr_3La_2(BO_3)_4$ under UV excitation, J. Lumin. 130 (2010) 483–487.

[8] C.T. Lee, F.S. Chen, C.H. Lu, Microwave-assisted solvothermal synthesis and characterization of SnO_2:Eu^{3+} phosphors, J. Alloys Compd. 490 (2010) 407–411.

[9] C.C. Lin, Y.S. Tang, S.F. Hu, R.S. Liu, $KBaPO_4$:Ln (Ln = Eu, Tb, Sm) phosphors for UV excitable white light-emitting diodes, J. Lumin. 129 (2009) 1682–1684.

[10] Y.S. Chang, F.M. Huang, Y.Y. Tsai, L.G. Teoh, Synthesis and photoluminescent properties of YVO_4:Eu^{3+} nano-crystal phosphor prepared by Pechini process, J. Lumin. 129 (2009) 1181–1185.

[11] S. Choi, Y.M. Moon, K. Kim, H.K. Jung, S. Nahm, Luminescent properties of a novel red-emitting phosphor: Eu^{3+}-activated $Ca_3Sr_3(VO_4)_4$, J. Lumin. 129 (2009) 988–990.

[12] A.A. Setlur, H.A. Comanzo, A.M. Srivastava, W.W. Beers, Spectroscopic evaluation of a white light phosphor for UV-LEDs—$Ca_2NaMg_2V_3O_{12}$:Eu^{3+}, J. Electrochem. Soc. 152 (2005) H205–H208.

[13] H. Yamamoto, S. Seki, J.P. Jeser, T. Ishiba, Thermal quenching of luminescence in a disordered compound: $EuNa_2Mg_2(VO_4)_3$, J. Electrochem. Soc. 127 (1980) 694–701.

[14] B.I. Lazoryak, T.V. Strunenkova, V.N. Golubev, E.A. Vovk, L.N. Ivanov, Triple phosphates of calcium, sodium and trivalent elements with whitlockite-like structure, Mater. Res. Bull. 31 (1996) 207–216.

[15] X. Wu, Y. Huang, L. Shi, H.J. Seo, Spectroscopy characteristics of vanadate $Ca_9Dy(VO_4)_7$ for application of white-light-emitting diodes, Mater. Chem. Phys. 116 (2009) 449–452.

[16] A.A. Belik, O.V. Yanov, B.I. Lazoryak, Synthesis and crystal structure of $Ca_9Cu_{1.5}(PO_4)_7$ and reinvestigation of $Ca_{9.5}Cu(PO_4)_7$, Mater. Res. Bull. 36 (2001) 1863–1871.

[17] I.A. Leonidov, L.L. Surat, O.N. Leonidova, R.F. Samigullina, System $Ca_3(VO_4)_2$–Na_3VO_4–$LaVO_4$, Russ. J. Inorg. Chem. 48 (2003) 1872–1877.

[18] Y.H. Zhou, J. Lin, Morphology control and luminescence properties of YVO_4:Eu phosphors prepared by spray pyrolysis, Opt. Mater. 27 (2005) 1426–1432.

[19] M. Yu, J. Lin, Z. Wang, J. Fu, S. Wang, H.J. Zhang, Y.C. Han, Fabrication, patterning, and optical properties of nanocrystalline YVO_4:A (A = Eu^{3+}, Dy^{3+}, Sm^{3+}, Er^{3+}) phosphor films via sol-gel soft lithography, Chem. Mater. 14 (2002) 2224–2231.

[20] C. Gorller-Walrand, K. Binnemans, Rationalization of crystal-field parametrization, in: K.A. Gschneidner, Jr., L. Eyring (Eds.), Handbook on the Physics and Chemistry of Rare Earths, vol. 23, North-Holland, Amsterdam, 1996.

[21] G. Blasse, B.C. Grabmaier, Lumin. Mater., Springer-Verlag, Berlin Heidelberg, 1994, p. 100, (chapter 4).

[22] Z.L. Wang, H.B. Liang, M.L. Gong, Q. Su, Luminescence investigation of Eu^{3+} activated double molybdates red phosphors with scheelite structure, J. Alloys Compd. 432 (2007) 308–312.

[23] B.I. Lazoryak, O.V. Baryshnikova, S.Yu. Stefanovich, A.P. Malakho, V.A. Morozov, A.A. Belik, I.A. Leonidov, O.N. Leonidova, G. Van Tendeloo, Ferroelectric and ionic-conductive properties of nonlinear-optical vanadate, $Ca_9Bi(VO_4)_7$, Chem. Mater. 15 (2003) 3003–3010.

[24] A.A. Belik, S.V. Grechkin, L.O. Dmitrienko, V.A. Morozov, S.S. Khasanov, B.I. Lazoryak, Crystal structures of double vanadates $Ca_9R(VO_4)_7$. IV. R = Er, Tm, Yb, and Lu, Crystallogr. Rep. 45 (2000) 896–901.

[25] R.A. Benhamou, A. Bessière, G. Wallez, B. Viana, M. Elaatmani, M. Daoud, A. Zegzouti, New insight in the structure–luminescence relationships of $Ca_9Eu(PO_4)_7$, J. Solid State Chem. 182 (2009) 2319–2325.

[26] G. Blasse, Luminescence of inorganic solids: from isolated centres to concentrated systems, Prog. Solid State Chem. 18 (1988) 79–171.

[27] B. Dickens, L.W. Schroeder, W.E. Brown, Crystallographic studies of the role of Mg as a stabilizing impurity in β-$Ca_3(PO_4)_2$. The crystal structure of pure β-$Ca_3(PO_4)_2$, J. Solid State Chem. 10 (1974) 232–248.